Modal Parameter Extraction Based on Hilbert Transform of Modal Responses

Zheng Min*, Shen Fan**

*College of Civil Aviation, Nanjing University of Aeronautics and Astronautics, China
**College of Aerospace Engineering, Nanjing University of Aeronautics and Astronautics, China
*zhengminsf@163.com, **shen0039@ntu.edu.sg

***Abstract*—Two modal identification methods based on Hilbert Transform of modal responses are used to extract modal parameters of a structure in this paper. First, the acceleration response time history polluted by noises is processed using Empirical Mode Decomposition with Singular Value Decomposition. Then, the frequencies and damping ratios of the system can be estimated by performing Hilbert Transform for obtained modal responses. The mode shapes can be achieved when the responses at all degrees of freedom are measured. The proposed methods are illustrated using a simulated airplane model with dense modes built in ADAMS (Automatic Dynamic Analysis of Mechanical Systems) software. The simulation results demonstrate that the outlined two methods based on Hilbert Transform can identify modal parameters well with the help of EMD and SVD as signal preprocessor even for the structure with the closely space modes, low-energy components.**

***Index Terms*—modal analysis, Hilbert transform, Empirical Mode Decomposition, signal processing**

I. INTRODUCTION

Modal analysis approach is an important tool for experimental identification of a structural dynamics models. Identified parameters can be used for design of active and passive control of structures and structural health monitoring [1].

There are numerous approaches that can be applied to extract modal parameters of structure. Traditionally, modal parameters are extracted by performing the reducing and curve-fitting procedures either on series of measured frequency response function or on time response, such as impulse response function [2] and free-decay response [3]. Recently modal analysis based on output-only, which has gained more and more attention, can be done by utilizing the correlation functions and power spectra of the operating data [4]. Some time–frequency analysis tools, such as Wigner–Ville distribution, Wavelet Transform (WT) and Hilbert–Huang Transform (HHT) [5] building on Empirical Mode Decomposition (EMD) and Hilbert spectral analysis (HSA) also have been used for system identification [6], damage detection [7]-[10] and etc [11]. For example, the vibration responses are processed using HHT for fault diagnosis [12-13], the damage features detection of composite aircraft wing-box structures [14] and health monitoring of civil structural models [15-16]. HHT technique is also proposed to identify multi-degree-of-freedom (MDOF) linear systems with intermittency criteria [17] or band-pass filtering on the measured free vibration time histories [18]. In this paper, two modal identifications based on Hilbert Transform with EMD and SVD as preprocessor are applied to extract modal parameters of a simulated airplane model with closely spaced modes built in ADAMS software for validating the modal identification capabilities.

II. MODAL PARAMTER IDENTIFICATION

A. Modal Response

Considering a multi-freedom system, we can describe the behaviours of the system by the equations of motion as

$$M(t)\ddot{X}(t)+C(t)\dot{X}(t)+K(t)X(t)=F(t) \qquad (1)$$

where $M(t)$ is the mass matrix, $C(t)$ is the damping matrix, $K(t)$ is the stiffness, $F(t)$ is the vector of random forcing function, $X(t)$ is the vector of random displacements.

Using a modal transformation

$$x(t) = \sum_{j=1}^{N} \phi_j q_j(t) \tag{2}$$

and the orthogonality of mode shapes, a set of equations in the modal co-ordinates can be given as follows

$$\ddot{q}_j(t) + 2\xi_j \omega_j \, \dot{q}(t) + \omega_j^2 q_j(t) = \phi_j^T F(t) / m_j \tag{3}$$

where $q_j(t)$ is the jth generalized modal co-ordinate, ξ_j and ω_j are, respectively, the jth modal damping ratio and modal frequency, ϕ_j is the jth modal vector, m_j is the jth modal mass.

With the assumption of the existence of normal modes, due to a single impulse input force $f_l(t)$ at the lth DOF, i.e. $f_l(t)=F_0\delta(t)$, for all $j \neq l$, (3) can be written as

$$\ddot{q}_j(t) + 2\xi_j \omega_j \, \dot{q}(t) + \omega_j^2 q_j(t) = 0 \tag{4}$$

and

$$\ddot{q}_j(t) = \frac{F_0 \phi_{lj} \omega_j}{m_j \sqrt{1-\xi_j^2}} e^{-\xi_j \omega_j t} \cos(\omega_{dj} t + \varphi_j + \frac{\pi}{2}) \tag{5}$$

where $\varphi_j = \tan^{-1}\left[2\xi_j \sqrt{1-\xi_j^2} \Big/ \left(1-2\xi_j^2\right) \right]$, ω_{dj} is the natural frequency, ϕ_{lj} is the modal participation factor.

The impulse acceleration response $\ddot{x}_p(t)$ at the pth DOF can be derived as

$$\ddot{x}_p(t) = \sum_{j=1}^{N} \phi_{pj} \, \ddot{q}_j(t) = \sum_{j=1}^{N} \ddot{x}_{pj}(t) \tag{6}$$

From (5) we can obtain

$$\ddot{x}_{pj}(t) = C_{pl,j} e^{-\xi_j \omega_j t} \sin\left(\omega_{dj} t + \vee_{pl,j}\right) \tag{7}$$

where

$$C_{pl,j} = \frac{F_0 \phi_{pj} \phi_{lj}}{m_j \omega_{dj}} \tag{8}$$

$$\vee_{pl,j} = \varphi_j + \phi_{pl,j} \tag{9}$$

and $\phi_{pl,j}$ is the phase difference between the pth element and the lth element in the jth mode shape.

B. Identifications of Natural Frequencies and Damping Ratios

Empirical Mode Decomposition (EMD) method [8] can extract the properties of signals even with nonlinear and non-stationary characteristics by decomposing any complicated data set via EMD into a finite, often small, number of Intrinsic Mode Functions (IMFs) that admit a well-behaved Hilbert transform. In this paper, EMD is applied to decompose the measured acceleration response excited by a multi-component loading with the impulse, harmonic and noise properties to obtain modal responses. Considering a system with an input signal applied to the lth DOF, the measured acceleration response $\ddot{z}_p(t)$ at the pth DOF can be processed as follows:

$$\ddot{z}_p(t) = \sum_{j=1}^{N} \ddot{x}_{pj}(t) + \sum_{g=1}^{G} \ddot{x}_{ph}(t) + \sum_{h=1}^{H} \ddot{x}_{po}(t) + \ddot{r}_p(t) \tag{10}$$

where $\ddot{x}_{pj}(t)$ are IMFs for impulse response components, $\ddot{x}_{ph}(t)$ are IMFs for harmonic components. The IMFs $\ddot{x}_{pj}(t)$ can be processed through the Hilbert transform to determine modal parameters of the system and $\ddot{x}_{ph}(t)$ can be identified as arising from harmonic excitation with zero damping.

The analytical signal $Y_{pj}(t)$ of $\ddot{x}_{pj}(t)$ is given

$$Y_{pj}(t) = \ddot{x}_{pj}(t) + i\tilde{\ddot{x}}_{pj}(t) \tag{11}$$

where $\tilde{\ddot{x}}_{pj}(t)$ is the Hilbert Transform of $\ddot{x}_{pi,j}(t)$.

Equation (11) also can be expressed as

$$Y_{pj}(t) = A_{pj}(t) e^{i\theta_{pj}(t)} \tag{12}$$

where A_{pj} is the instantaneous amplitude and θ_{pj} is the instantaneous phase angle. Instantaneous modal parameters can be obtained through the two identification methods below.

Method 1

For a special case in which $\xi_j(t) / \omega_j(t)$ is very small, one can obtain

$$A_{pj}(t) = C_{pl,j} e^{-\xi_j \omega_j t} \tag{13}$$

$$\theta_{pj}(t) = \omega_{dj} t + \vee_{pl,j} + \frac{\pi}{2} \tag{14}$$

We can get the first derivatives of the above equations vs time t as [18]

$$\frac{d \ln A_{pj}(t)}{dt} = -\xi_j(t)\omega_j(t) \tag{15}$$

$$\frac{d\theta_{pj}(t)}{dt} = \omega_{dj}(t) = \omega_j(t)\sqrt{1-\xi_j^2(t)} \tag{16}$$

Equation (15) and (16) can be simplified as the following

$$\varepsilon_1(t) = -\xi_j(t)\omega_j(t) \tag{17}$$

$$\varepsilon_2(t) = \omega_j(t)\sqrt{1-\xi_j^2(t)} = \omega_{dj}(t) \tag{18}$$

The damping ratio $\xi_j(t)$ can be identified from

$$\xi_j(t) = \sqrt{\frac{\varepsilon_1^2(t)}{\varepsilon_1^2(t)+\varepsilon_2^2(t)}} \tag{19}$$

And the damped natural frequency $\omega_{dj}(t)$ can be obtained from $\varepsilon_2(t)$.

Method 2

Multiplying (4) by ϕ_{pj} leads to

$$\ddot{x}_{pj}(t) + 2\xi_j(t)\omega_j(t)\dot{x}_{pj}(t) + \omega_j^2 x_{pj}(t) = 0 \tag{20}$$

Further, according to (11), we can derive [19]

$$\ddot{Y}_{pj}(t) + 2\xi_j(t)\omega_j(t)\dot{Y}_{pj}(t) + \omega_j^2 Y_{pj}(t) = 0 \tag{21}$$

and

$$\ddot{\tilde{x}}_{pj}(t) + 2\xi_j(t)\omega_j(t)\dot{\tilde{x}}_{pj}(t) + \omega_j^2 \tilde{x}_{pj}(t) = 0 \tag{22}$$

Solving the equations of (20) and (22), instantaneous modal frequencies $\omega_j(t)$ and damping ratios $\xi_j(t)$ can be achieved from the following

$$\omega_j^2(t) = \omega_{dj}^2(t) - \frac{A''_{pj}(t)}{A_{pj}(t)} + 2\frac{A'^2_{pj}(t)}{A^2_{pj}(t)} + \frac{A'^2_{pj}(t)\omega'_{dj}(t)}{A^2_{pj}(t)\omega_{dj}(t)}$$

$$= \frac{\tilde{\ddot{x}}''_{pj}(t)\ddot{x}'_{pj}(t) - \ddot{x}''_{pj}(t)\tilde{\ddot{x}}'_{pj}(t)}{\ddot{x}_{pj}(t)\tilde{\ddot{x}}'_{pj}(t) - \tilde{\ddot{x}}_{pj}(t)\ddot{x}'_{pj}(t)} \tag{23}$$

$$\xi_j(t) = -\frac{A'_{pj}(t)}{A_{pj}(t)} - \frac{\omega'_{dj}(t)}{2\omega_{dj}(t)}$$

$$= \frac{1}{2}\frac{\tilde{\ddot{x}}_{pj}(t)\ddot{x}''_{pj}(t) - \ddot{x}_{pj}(t)\tilde{\ddot{x}}''_{pj}(t)}{\ddot{x}_{pj}(t)\tilde{\ddot{x}}'_{pj}(t) - \tilde{\ddot{x}}_{pj}(t)\ddot{x}'_{pj}(t)}\frac{1}{\omega_j(t)} \tag{24}$$

where $\omega_{dj}(t)=d\theta_{pj}(t)/dt$, $\ddot{x}'_{pj}$ and $\ddot{x}''_{pj}$ are the first and second derivative of $\ddot{x}_{pj}(t)$ respectively, $\tilde{\ddot{x}}'_{pj}(t)$ and $\tilde{\ddot{x}}''_{pj}(t)$ are the first and second derivative of $\tilde{\ddot{x}}_{pj}(t)$ respectively.

C. Identification of Mode Shapes

According to (8) and (13), the ratio of the absolute value of the modal elements ϕ_{pj} and ϕ_{qj} can be written as

$$\phi_{pj} / \phi_{qj} = A_{pj}(t_0) / A_{qj}(t_0) \tag{25}$$

where $A_{pj}(t_0)$ and $A_{qj}(t_0)$ are, respectively, the magnitudes at the time $t=t_0$ of the average least-square straight lines for the decaying amplitudes $A_{pj}(t)$ and $A_{qj}(t)$ obtained previously.

With the existence of normal modes, all the mode shapes are real. From (9) and (14), the phase difference $\phi_{pq,j}$ between the pth element and the qth element in the jth mode shape can be given by

$$\phi_{pq,j} = \bar{\theta}_{pj}(t_0) - \bar{\theta}_{qj}(t_0) \tag{26}$$

where $\bar{\theta}_{pj}(t_0)$ and $\bar{\theta}_{qj}(t_0)$ are, respectively, the magnitudes of the average least-square straight lines for the phase angles $\theta_{pj}(t)$ and $\theta_{qj}(t)$ at the time $t=t_0$ obtained previously. The mode shapes can be achieved when the responses at all degrees of freedom are measured.

III. Simulated Experimental Case Study

The outlined two methods based on Hilbert Transform are applied to analyze the response data acquired from a simulated test conducted in ADAMS. The modal parameters are extracted and compared with those from ADAMS software.

A. Description of Test Structure and Tests

An airplane model with closely spaced modes built in ADAMS is considered. It is made of iron and five millimeters thick. The model was fixed at the coordinate origin. The acceleration responses were measured only in the vertical direction at 27 points for vertical excitation at two symmetrical excitation points on the wingtip. Fig.1 shows the test model and the distribution of the 27 measurement points. The location numbers were arranged counterclockwise with the beginning of airplane head.

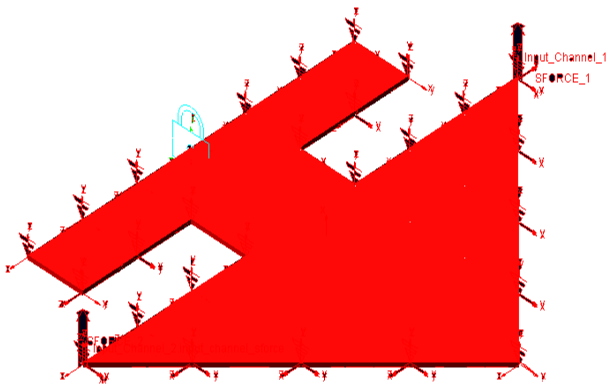

Fig. 1. Airplane model built in ADAMS with indication of the distribution of measurement points

An input signal with the multi-component properties, which is composed of a sinusoidal harmonic frequency at 80 Hz and an impulse at the moment of 0.1 second along with the stationary white noise, was applied to the 2 excitation points. Fig.2 shows the time history of the excitation signal.

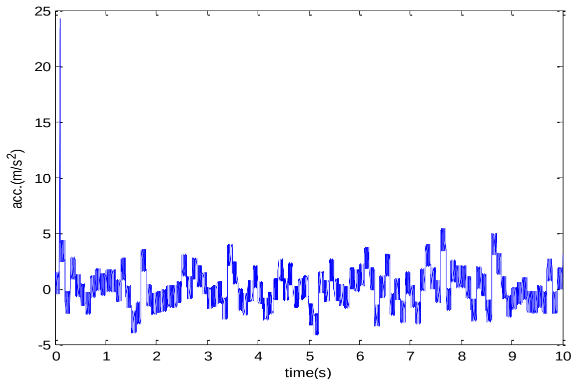

Fig. 2. Time history of the excitation signal

A total of 5000 response samples corresponding to signal duration of 10s with a sampling rate of 500 Hz at the 27 locations were acquired simultaneously, which results in a bandwidth of 0–250 Hz. Fig.3 shows the temporal waveform of the 9th location and its FFT spectrum, respectively.

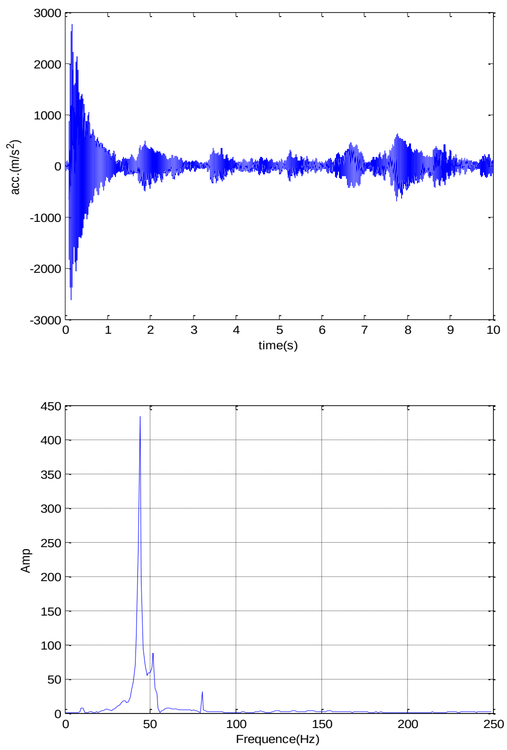

Fig. 3. Time history and FFT spectrum of measured acceleration response at the 9th location of the airplane model

B. Signal Processing

In practical applications, the closely space modes usually occur on some engineering structures. It is quite challenging to extract characteristic parameters for such structures. SVD filtering is used to help EMD separate the dense modes in this paper.

The SVD-decomposed subspaces are an orthogonal representation of the original space, the relevant discrete time series $y_w(k)$ (w=1,2,…s) corresponding to the subspace w should have strong correlation with the original signal. With the aid of the correlation coefficients, a screening process will be conducted and the selected vital time series $y_w(k)$ will be remained.

After reconstructing the signal $y_{rec}(k)$ by superposing the retained time series $y_w(k)$ as following

$$y_{rec}(k) = \sum_{w=1}^{s} y_w(k) \tag{27}$$

We process it through the band-pass filters each with a frequency band near the possible frequencies of the system. Each filtered time history is decomposed by EMD, and the resulting first IMFs will be processed through the Hilbert transform for the identification of modal parameters [18].

The modal responses near the natural frequencies are shown in Fig.4. It can be seen that the 5th selected component at 19 Hz that contains low-energy component and the two closed space frequencies near the 3th selected component at 52 Hz and the 2nd selected component at 54 Hz are clearly visible. It is noted that a segment of the modal response near t =0 is not a decaying function mainly due to the phase shift. Such a segment should be removed before the Hilbert transform is applied to these modal responses to extract modal parameters of the system.

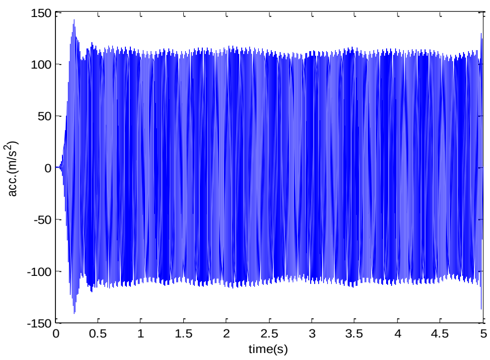

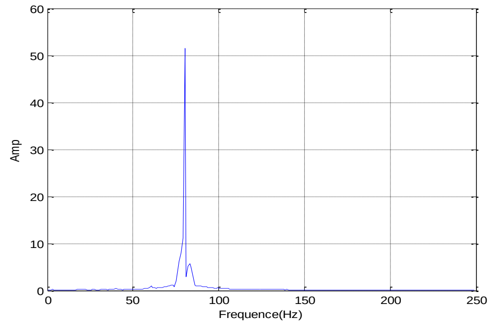

（a）Time history and FFT spectrum of the 1st selected component

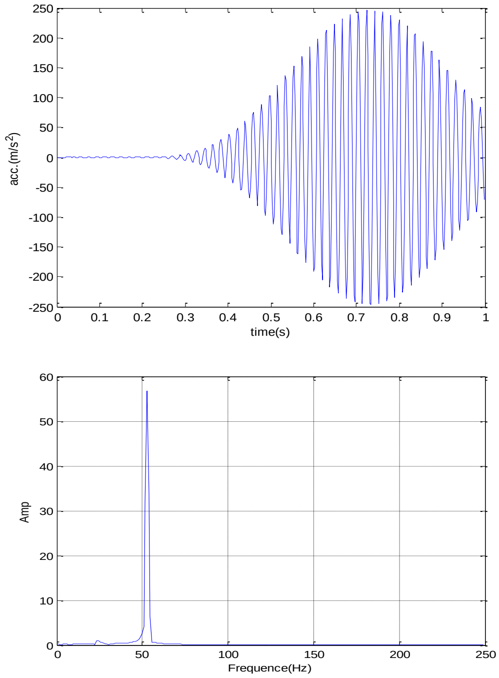

（b）Time history and FFT spectrum of the 2nd selected component

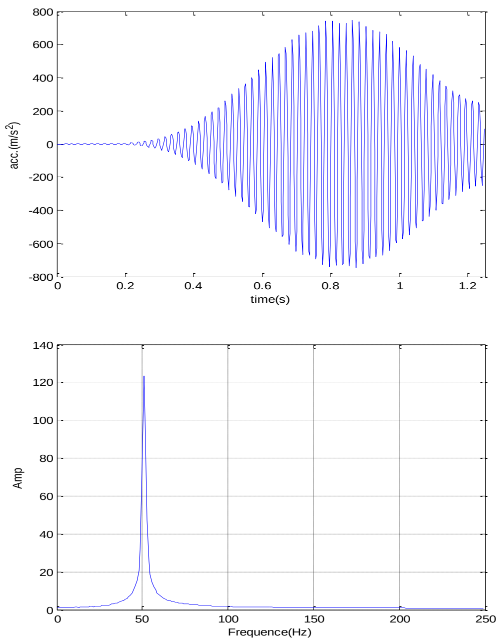

（c）Time history and FFT spectrum of the 3rd selected component

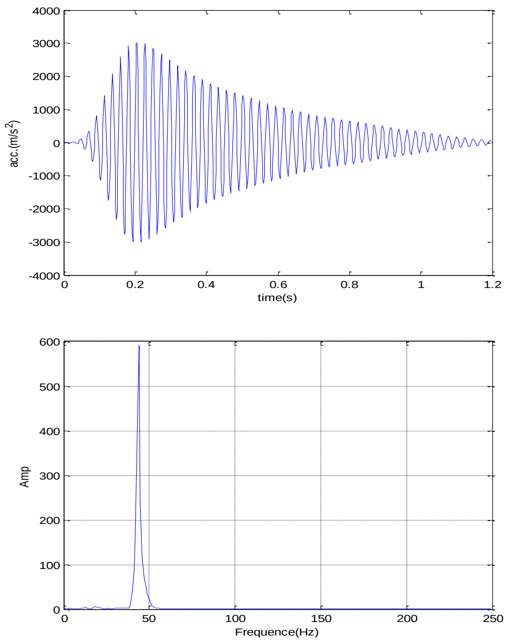

（d）Time history and FFT spectrum of the 4th selected component

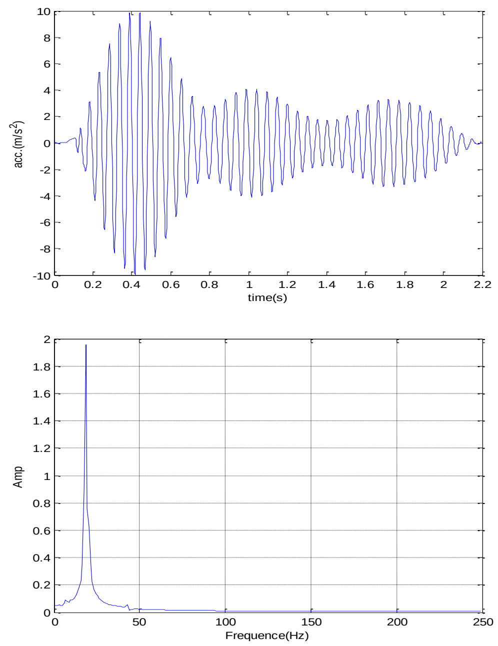

（e）Time history and FFT spectrum of the 5th selected component

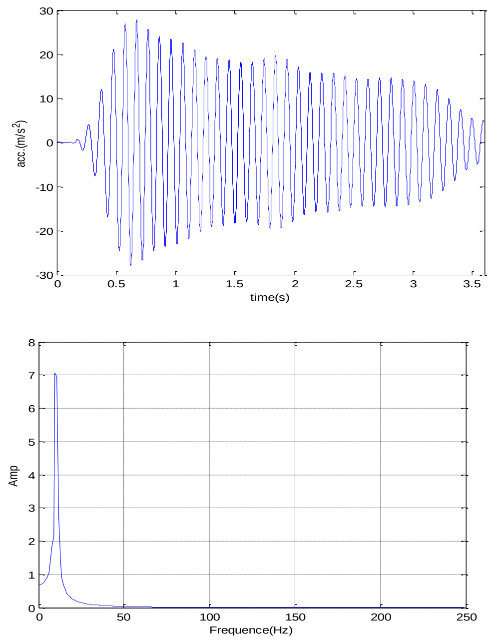

（f）Time history and FFT spectrum of the 6th selected component

Fig. 4. Achieved modal responses at the 9th location through the proposed signal processing technique

C. Modal Identification

In order to avoid the bad influences of the phase shift during band-pass filtering and end effects of EMD on identified results, after removing the segment from t =0 to the maximum amplitude each modal response were processed through the Hilbert transform to determine the instantaneous amplitude and instantaneous phase. The identified results based on the response at 9th position and the baseline models from ADAMS are listed in Table 1 for comparison purposes.

TABLE I THE IDENTIFIED FREQUENCIES AND DAMPING RATIOS

Mode No.	Frequencies(Hz)			Damping Ratios(%)		
	Base Model	Method 1	Method 2	Base Model	Method 1	Method 2
1	10.269	10.271	10.282	0.59	0.61	0.70
2	19.036	18.833	18.759	0.62	0.68	0.81
3	43.667	43.728	43.840	1.03	1.10	1.15
4	51.717	50.797	50.736	1.49	1.27	1.21
5	53.794	52.855	52.936	1.16	1.25	1.33
6	80	79.998	80.053	0	0.02	0.01

In Table 1, we read that the identified harmonic frequencies are 79.998 Hz and 80.053 Hz with corresponding damping ratios of 0.02% and 0.01% in method 1 and 2 respectively. Note that, although the damping should be zero in theory, it is very small in the results and therefore an analyst could hardly be misled this pole as a true eigenpole of the system. The results also demonstrate that the proposed methods in this paper can identify the modal frequencies with great accuracy and the corresponding damping ratios even when the dense modal frequencies exist near 52Hz. The modal parameters near the frequencies of 10Hz and 19Hz with the low-energy, which are not clear in the FFT spectra of Fig.3, were extracted well. Generally, the damping ratios from method 2 were less accurate than those from method 1.

The results from the responses of other locations alone are very close to those based on the 9th one. With the acceleration responses at all positions measured, the mode shapes of the system can be extracted. The achieved mode shapes are visualized in Fig.5 with the theoretical mode shapes for comparison. It is observed that the identified results have a good agreement with the baseline model.

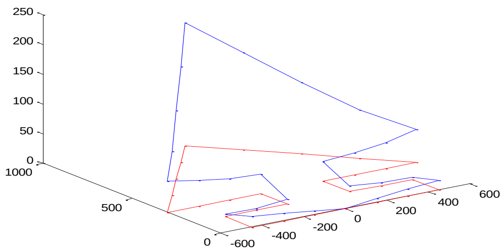

（a）The 1st mode shapes

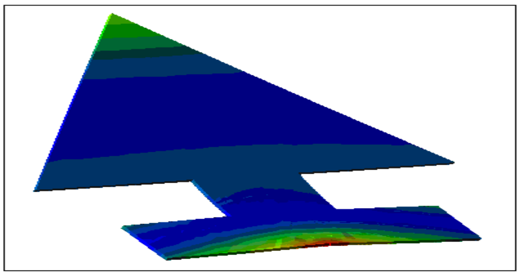

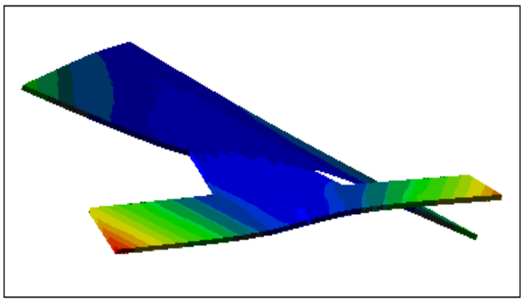

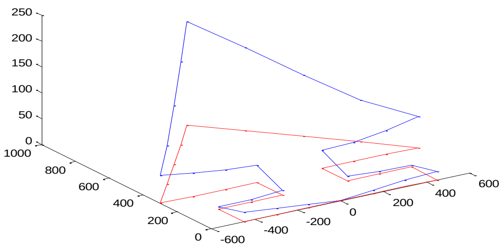

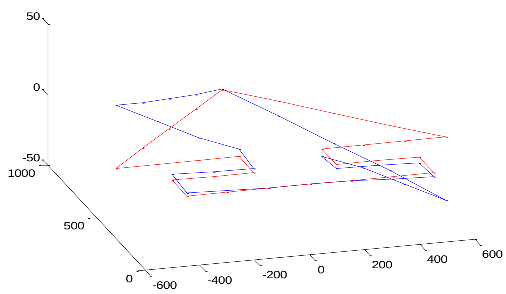

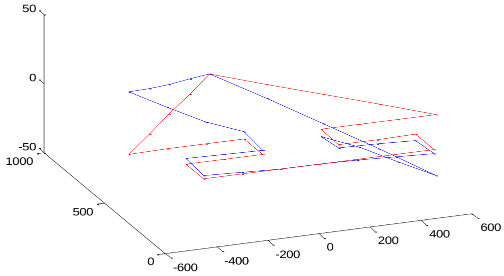

（b）The 2nd mode shapes

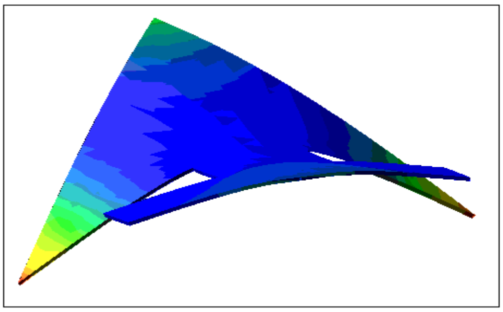

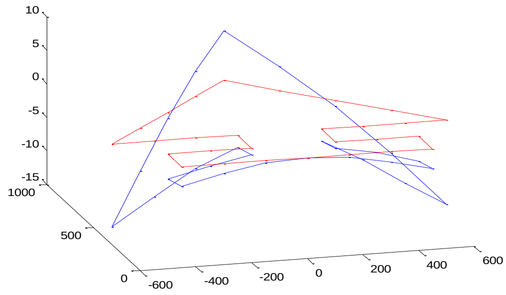

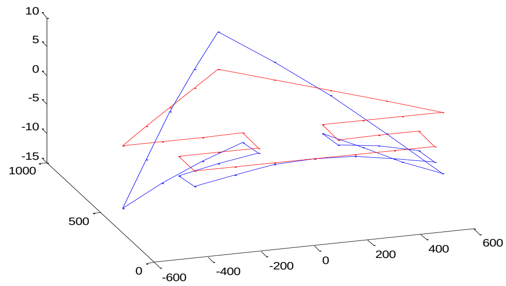

（c）The 3rd mode shapes

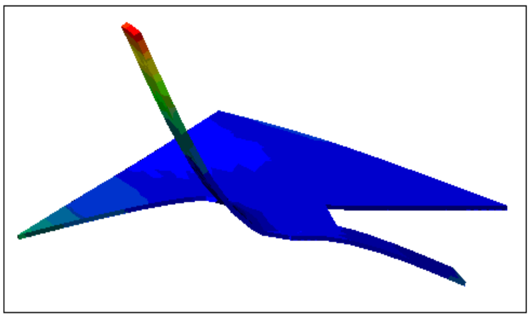

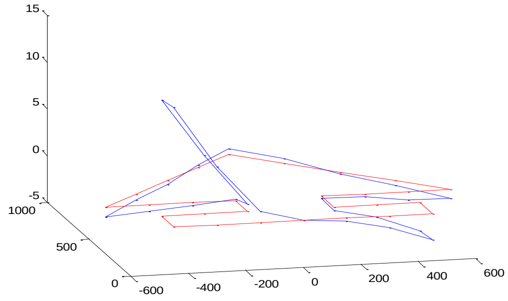

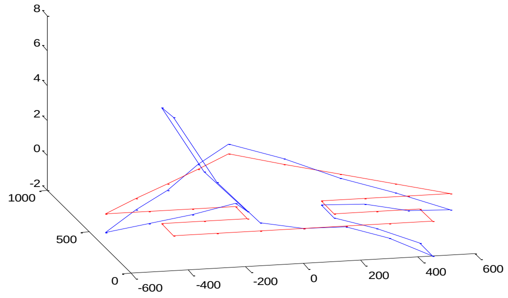

（d）The 4th mode shapes

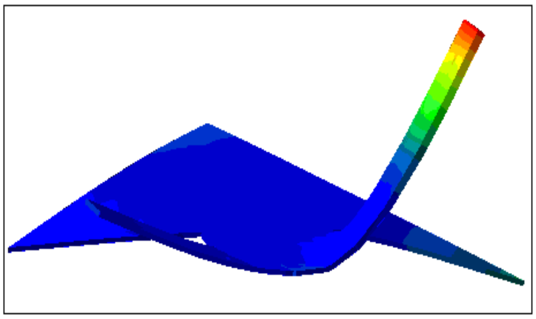

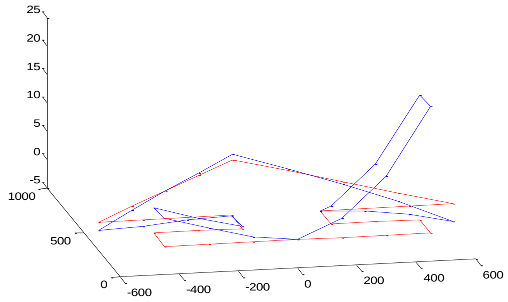

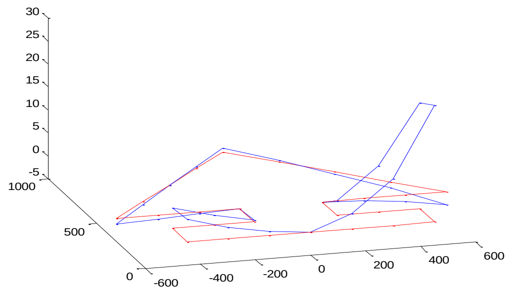

（e）The 5th mode shapes

Fig. 5. Identified mode shapes from the measured responses

(upper-ADAMS, middle-Method1, lower-Method2)

IV. CONCLUSION

In this study, two identification methods of structural dynamic characteristics based on the Hilbert Transform of modal responses have been illustrated through an airplane model example built in ADAMS. The results demonstrate that with the EMD and SVD as preprocessors both of the outlined methods offer effective tools for yielding modal parameters even if dense modes and low-energy component exist. When the harmonic excitations are present, the dynamic response will include the associated forced harmonic components which can be seen as virtual non-damped modes. These virtual modes can be achieved easily through the proposed identifications. Further investigation can be made of modal identification for practical large structures.

ACKNOWLEDGMENT

This work has been funded by National Natural Science Foundation of China (61179056).

REFERENCES

[1] R. Segawa, S. Yamamoto, A. Sone, A. Masuda, "Cumulative damage estimation using wavelet transform of structural response," in *Proceedings of 12th World Conference on Earthquake Engineering*, Auckland, New Zealand, 2000, pp.1212–1220.

[2] K. Yua, J. Yea, J.X. Zoua, B. Yangb, H. Yang. "Missile flutter experiment and data analysis using wavelet transform," *Journal of Sound and Vibration*, vol.269, no.3-5, pp.899–912, Jan.2004.

[3] T.P. Le, P. Argoul. "Continuous wavelet transform for modal identification using free decay response," *Journal of Sound and Vibration*, vol.277, no.1-2, pp.73–100, 2004.

[4] F. Shen, M. Zheng, D.F. Shi, F. Xu. "Using the cross-correlation technique to extract modal parameters on response-only data," *Journal of Sound and Vibration*, vol.259, no.5, pp.1163–1179, Jan. 2003.

[5] J.S. Chen, "Signal filtering using the Hilbert-Huang Transform," *Journal of Science and Engineering Technology*, vol. 6, no.1, pp. 75–84, 2010.

[6] A. Chakrabortya, B. Basua, M. Mitrab, "Identification of modal parameters of a mdof system by modified L–P wavelet packets," *Journal of Sound and Vibration*, vol.295, pp.827–837, Aug.2006.

[7] A. Sone, S. Yamamoto, A. Masuda, "Detection of inelastic excursions in hysteretic systems for cumulative damage estimation using wavelet transform of response time histories," in *Proceedings of 12th World Conference on Earthquake Engineering*, Auckland, New Zealand, 2000, pp.1220–1228.

[8] S.R. Qina, Y.M. Zhong, "A new envelope algorithm of Hilbert–Huang Transform," *Mechanical Systems and Signal Processing*, vol.20, no.8, pp.1941–1952, Nov.2006.

[9] Z.K. Penga, Peter W. Tsea, F.L. Chu, "A comparison study of improved Hilbert–Huang transform and wavelet transform: Application to fault diagnosis for rolling bearing," *Mechanical Systems and Signal Processing*, vol.19, no.5, pp.974–988, 2005.

[10] N.E. Huang, M.L. Wu, Wendong Qu, Steven R. Long and Samuel S. P. Shen, "Applications of Hilbert–Huang transform to non-stationary financial time series analysis," *Applied Stochastic Models in Business and Industry*, vol.19, no.3, pp.245–268, Jul.2003.

[11] N.Padmaja, S.Varadarajan, R.Swathi, "Signal processing of radar echoes using wavelets and Hilbert Huang Transform," *Signal & Image Processing: An International Journal (SIPIJ)*, vol.2, no.3, Sep. 2011.

[12] Z.N. Han, J.X. Gao, "Gear local fault diagnosis with empirical mode decomposition and Hibert Huang Transform," *Advanced Materials Research*, vol.199-200, pp.899–904, Feb.2011.

[13] Z.Y. Su, Y.M. Zhang, M.P. Jia, F.Y. Xu and J.Z. Hu, "Gear fault identification and classification of singular value decomposition based on Hilbert-Huang transform," *Journal of Mechanical Science and Technology*, vol.25, no.2, pp.267–272, Feb.2011.

[14] H.G. Chen, Y.J. Yan, J.S. Jiang, "Vibration-based damage detection in composite wing box structures by HHT," *Mechanical Systems and Signal Processing*, vol.21, no.1, pp.307–321, Jan.2007.

[15] D. Pinesa, L. Salvino, "Structural health monitoring using empirical mode decomposition and the Hilbert phase," *Journal of Sound and Vibration*, vol.294, no.1-2, pp.97–124, Jun.2006.

[16] A. Atul, M.R. Rama, K. Lakshmi, M.P. Mathews, "Hilbert Huang Transform combined with wavelet packet based sifting for structural health monitoring," *International Journal of Earth Sciences and Engineering*. vol.4, n.6, pp. 472–475, Oct. 2011.

[17] H.L. Li, L.H. Yang, D.R. Huang, "The study of the intermittency test filtering character of Hilbert–Huang transform," *Mathematics and Computers in Simulation*, vol.70, no.1, pp.22–32, Sep.2005.

[18] J.N. Yang, Y. Lei, S.W. Pan, N. Huang, "System identification of linear structures based on Hilbert–Huang spectral analysis. Part 1: normal modes," *Earthquake Engineering and Structural Dynamics*, vol.32, no.10, pp.1443–1467, Jul.2003.

[19] J. Xiao, "Study on time-frequency analysis of modal identification for time-varying system," M.S. thesis, College of Civil Aviation, Nanjing University of Aeronautics and Astronautics, Nanjing, China, Mar.2006.

[20] M.J. Brenner, "Non-stationary dynamics data analysis with wavelet-SVD filtering," *Mechanical Systems and Signal Processing*, vol.17, no.4, pp.765–786, Jul.2003.

Zheng Min joined Nanjing University of Aeronautics and Astronautics in 2002 as an academic staff. She became a Member of Chinese Society of Aeronautics and Astronautics in 2006. She went to National University of Singapore as a research fellow in 2008. She achieved his PhD degree at College of Aerospace Engineering in Nanjing University of Aeronautics and Astronautics in 2000. Her research interests include structure dynamics, signal processing and energy efficiency.